Strongly disordered chain of impedances: theoretical analysis and numerical results

1990 J. Phys. A: Math. Gen. 23 1085

(http://iopscience.iop.org/0305-4470/23/7/015)

J. Phys. A: Math. Gen. 23 (1990) 1085–1100. Printed in the UK

Strongly disordered chain of impedances: theoretical analysis and numerical results

J P Hulin†, J P Bouchaud‡ and A Georges§

† Laboratoire d'Hydrodynamique et de Mécanique Physique, unité associée au CNRS, ESPCI, 10 Rue Vauquelin, 75231 Paris Cedex 05, France
‡ Laboratoire de Physique Statistique de l'ENS, associé au CNRS, 24 rue Lhomond, 75231 Paris Cedex 05, France
§ Laboratoire de Physique Théorique de l'ENS, associé au CNRS et à l'université de Paris Sud, 24 rue Lhomond, 75231 Paris Cedex 05, France

Received 13 September 1989

Abstract. We study the input impedance of a chain of random resistors chosen according to a 'broad' distribution (i.e. decaying as a power law for large arguments). As a function of frequency, the modulus of the input impedance varies as a power law, while its phase has a well defined value. A simple theoretical analysis, based on estimations of sums of random variables, yields the value of the exponents which are in perfect agreement with numerical simulations, even when logarithmic corrections come into play. The analysis can be extended further to investigate the sample to sample fluctuations of the impedance. Again, agreement with simulations is very good.

1. Introduction

Asymptotically non-Gaussian diffusion or dispersion represents the simplest example of a non-mean-field (critical) phenomenon [1, 2]. The two basic mechanics responsible for such behaviour are:

(a) the presence of broadly distributed events, for which some of the moments (for example their mean or their variance) fail to exist;

(b) the presence of *long range* correlations—which are usually self induced—associated with the lack of a characteristic length or time scale [2].

A very simple example of a non-diffusive random walk is provided by a one-dimensional line with a broad distribution of either the local (symmetrical) hopping rates (case A) or the local trapping times (case B): this corresponds, in an electrical analogue, to a chain of impedances (see figure 1) containing an anomalously large

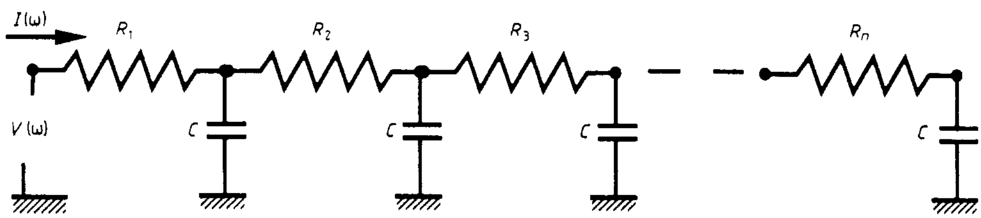

Figure 1. One-dimensional chain of impedances with random resistors.

number of either high resistances (A) or large capacitances (B). In this diffusion problem, we seek to determine the probability $P(n, t)$ for the presence of a particle at site number n: the corresponding variable in the electrical analogy is the distribution of charges in the chain.

In this paper, we study the chain of impedance cells represented in figure 1 (all the capacitances are equal to a value C); the values R_n of the resistors are chosen at random according to the algebraic law:

$$\rho(R)=\mu/R_0(R_0/R)^{(1+\mu)} \qquad (\mu>0) \qquad \text{for } R>R_0 \tag{1a}$$

$$\rho(R)=0 \qquad \text{for } R<R_0. \tag{1b}$$

$\rho(R)\,\mathrm{d}R$ is the probability for a given resistor to have a value between R and $R+\mathrm{d}R$. The quantities of interest are as follows.

For the diffusion problem: the time dependence of the typical position of the diffusing objects, the full shape $P(n, t)$ of the diffusion front and its fluctuations [see 2, ch II]

For the electrical problem, the variations with the frequency ω of the end-to-end impedance (i.e. the ratio of the input voltage to the output current) and of the complex admittance $A(\omega)$ (i.e. the ratio of the input current to the input voltage). This latter quantity strongly depends on the *particular realisation of the disorder*. We shall thus study here the average of the *logarithm* of the admittance, leading to a well defined amplitude and phase. The mean value and the *fluctuations* of the phase will also be discussed.

2. Theoretical background

If (and only if) only the resistors are random, a powerful theorem [2, 3] (valid for all lattice dimensionalities) states that the infinite time diffusion coefficient D (if it exists) is proportional to the *zero frequency* average end-to-end conductance σ. Nevertheless, as we shall show now, the properties of the diffusion problem can be used to obtain information on the electrical network even at finite frequencies or when D is zero (anomalous diffusion).

For the problem considered here, the average conductance σ in the limit of an infinitely long chain of impedance cells may or may not exist, depending on the value of μ.

For $\mu>1$, σ is finite and equal to

$$\sigma^{-1}=\lim_{L\to\infty}\frac{1}{L}\sum_{i=0}^{L}R_i=\langle R\rangle=\int_0^\infty R\rho(R)\,\mathrm{d}R<+\infty. \tag{2}$$

In contrast, for $\mu<1$, $\langle R\rangle$ is infinite and $\sigma(L)$ goes to zero as the length L of the chain tends towards infinity. Let us limit ourselves to a finite number L of elements and estimate *the largest resistor* $R_{\max}(L)$ among them: then we shall use $R_{\max}(L)$ as the upper bound in the integral of equation (2) which will give an effective mean value of the resistance for a chain of finite length. Using equation (1), the probability $P_+(R_{\max})$ that one resistor is larger than a value $R_{\max}$ is

$$P_+(R_{\max})=\int_{R_{\max}}^\infty \rho(R)\,\mathrm{d}R\approx(R_0/R_{\max})^\mu.$$

Therefore, in a series of L resistors, the largest value $R_{\max}$ is such that [4, 2 (appendix B)]

$$P_+(R_{\max})L \approx 1 \qquad \text{so that} \qquad R_{\max}(L) \propto L^{1/\mu}.$$

Thus:

$$\sigma^{-1}(L) = \frac{1}{L}\sum_{i=0}^{L} R_i \approx \int_{R_0}^{R_{\max}} R\rho(R)\,\mathrm{d}R \propto \int_{R_0}^{CL^{1/\mu}} R^{-\mu}\,\mathrm{d}R.$$

Hence, provided that $R_{\max} \gg R_0$:

$$\sigma^{-1}(L) \propto L^{1/\mu - 1} \qquad \text{for } \mu < 1 \tag{3a}$$

$$\sigma^{-1}(L) \propto \log L \qquad \text{for } \mu = 1. \tag{3b}$$

More precisely, $L\sigma^{-1}(L)/L^{1/\mu}$ has a limit distribution when $L \to \infty$ which is a Levy (stable) law: see section 4 and [4, 2 (appendix B)].

If diffusion has taken place over a finite length x after a time lapse t, one can define an effective 'finite size diffusion coefficient' $D(x)$ by

$$x^2 = D(x)t. \tag{4}$$

The proportionality between D and σ resulting from the theorem discussed above can be argued to hold for $D(x)$ and $\sigma(x)$ so that one obtains by taking $x = aL$ in equations ($3a, b$) (a being the length of one cell):

$$D(x) \propto \sigma(x) \propto x^{1-1/\mu} \qquad \text{for } \mu < 1 \tag{5a}$$

$$D(x) \propto \sigma(x) \propto (\log x)^{-1} \qquad \text{for } \mu = 1. \tag{5b}$$

Therefore the diffusion distance x of a particle in such a medium satisfies

$$x \propto t^{\mu/(1+\mu)} \qquad \text{for } \mu < 1 \tag{6a}$$

$$x \approx \sqrt{t/\ln t} \qquad \text{for } \mu = 1 \tag{6b}$$

$$x \propto t^{1/2} \qquad \text{for } \mu > 1. \tag{6c}$$

In the latter case $\sigma(x)$ reaches a constant value independent of x as soon as x is large enough and one has a normal diffusion law; on the other hand, for $\mu \leqslant 1$, diffusion is anomalously slow ($x < t^{1/2}$). The results of equation (6) are exact, as can be checked by a variety of other methods [5, 6], and coincide in one dimension with the one obtained for diffusion among traps (e.g. capacitances) with trapping times distributed according to a law: $\rho(\tau) \propto \tau^{-(1+\mu)}$.

If one now turns to the random resistor chain, the diffusion law (6) essentially means that, if the input voltage oscillates at a frequency ω, the charges move into *the chain* only up to a *penetration depth* $\lambda(\omega)$ such that:

$$\begin{aligned} &\lambda(\omega) \propto \frac{1}{\omega^{\mu/(1+\mu)}} && (\mu < 1) \\ &\lambda(\omega) \propto \sqrt{(\omega \ln \omega_0/\omega)^{-1}} && (\mu = 1) \\ &\lambda(\omega) \propto \frac{1}{\sqrt{\omega}} && (\mu > 1). \end{aligned} \tag{7}$$

One obtains equations (7) by taking $\omega = 1/t$ in equations (6) and taking for ω_0 the highest characteristic frequency in the problem: in our case, ω_0 is of order of $1/R_0C$.

Let us measure the admittance $A(\omega)$ of the chain of resistors and capacitors between its input and the ground connection (figure 1): the chain appears as a combination of $\lambda(\omega)/a$ random resistors in series and $\lambda(\omega)/a$ constant capacitors in parallel. For $\mu \geqslant 1$, the total resistive part is

$$\frac{\lambda(\omega)}{a}\sigma^{-1}\left(\frac{\lambda(\omega)}{a}\right)$$

where the effective mean resistance $\sigma^{-1}(\lambda(\omega)/a)$ is given by equation (3). Then, using equation (7) to compute $\lambda(\omega)$:

$$\operatorname{Re} A(\omega) \propto \frac{1}{\lambda(\omega)}\sigma\left(\frac{\lambda(\omega)}{a}\right) \propto \omega^{1/(1+\mu)} \qquad \text{for } \mu < 1 \qquad (8a)$$

$$\operatorname{Re} A(\omega) \propto \frac{1}{\lambda(\omega)\ln\lambda(\omega)} \propto \left(\frac{\omega}{\ln \omega_0/\omega}\right)^{1/2} \qquad \text{for } \mu = 1 \qquad (8b)$$

for $\mu > 1$, Re $A(\omega)$ is of the order of $\lambda(\omega)$ times the mean resistance $\langle R \rangle$ in the chain which is, in this case, independent of ω so that, from equation (7),

$$\operatorname{Re} A(\omega) \propto 1/\lambda(\omega) \propto \omega^{1/2}. \qquad (8c)$$

Since all capacitors are identical, the reactive part of the admittance simply verifies

$$\operatorname{Im} A(\omega) \approx \lambda(\omega) C\omega$$

so that, using again equations (7):

$$\operatorname{Im} A(\omega) \propto \omega^{1/1+\mu} \qquad \text{for } \mu < 1 \qquad (9a)$$

$$\operatorname{Im} A(\omega) \propto \left(\frac{\omega}{\ln \omega_0/\omega}\right)^{1/2} \qquad \text{for } \mu = 1 \qquad (9b)$$

$$\operatorname{Im} A(\omega) \propto \omega^{1/2} \qquad \text{for } \mu > 1. \qquad (9c)$$

All the equations (8) and (9) have to be understood in the sense of *typical* value, which here should be identified with the behaviour of $\exp[\langle \ln A \rangle]$.

We have thus shown, using simple arguments on sums of broadly distributed variables, that the admittance of a highly disordered chain scales with an anomalous power of the frequency when $\mu < 1$. These arguments provide the value of the exponent α and show that the real and imaginary part of the admittance follow the same scaling law with frequency given by equations (8) and (9).

As shown very elegantly by Mitescu *et al* [7, 13], one can relate the phase φ of the complex admittance $A(\omega)$ to the exponent α by using the analyticity properties of $A(\omega)$: the relation applies to all networks containing resistors, capacitors and inductors in any kind of pattern and its physical meaning is similar to that of the Kramers–Kronig relations. The key point is that, in the equations relating the complex voltages and intensities in the network, the frequency ω appears only through the product $\mathrm{j}\omega$ (the complex admittances of a capacitor and an inductance are respectively $1/\mathrm{j}C\omega$ and $\mathrm{j}L(\omega)$. These j factors are the only complex coefficients appearing in the relation; therefore, the admittance $A(\omega)$ between two points (figure 1) verifies: $A(\omega) = f(\mathrm{j}\omega)$ where f is a real function (containing only real parameters) of the complex variable $\mathrm{j}\omega$. If $|A(\omega)|$ is proportional to a power ω^α of ω in a given range of frequencies, then necessarily:

$$A(\omega) = |A(\omega)|\, \mathrm{e}^{\mathrm{j}\varphi} = A_0(\mathrm{j}\omega)^\alpha = A_0\, \mathrm{e}^{\mathrm{j}\psi}\omega^\alpha$$

and

$$\varphi = \alpha \frac{\pi}{2} \tag{10}$$

where A_0 is a *real* constant and φ is the phase of the complex admittance $A(\omega)$. Then:

$$\varphi = \frac{\pi}{4} \qquad \text{if } \alpha = 1/2 \text{ (as for } \mu > 1) \tag{11a}$$

$$\varphi = \frac{\mu}{1+\mu} \frac{\pi}{2} \qquad \text{if } \alpha = \frac{\mu}{1+\mu} \text{ (as for } \mu < 1). \tag{11b}$$

The *phase* φ is thus entirely determined by the diffusion exponent except for $\mu = 1$; in this case, one expects the phase to vary with frequency since no exact power law is verified.

Before going into the numerical part of this work, let us comment on the interest of investigating this model.

(a) It represents a 'toy model' for which the anomalous behaviour of the admittance, occurring in other more complex situations (such as for 2D percolation networks [8, 13] and in acoustic experiments on rocks or for conducting polymers) can be fully understood by simple arguments. One could have obtained expressions (8, 9) in another way by using a *scaling* assumption on $A(\omega, L)$:

$$A(\omega, L) = A(0, L) f(\lambda(\omega)/L)$$

and by requiring that, for $\lambda(\omega) \ll L$, $A(\omega, L)$ no longer depends on L. The fact that the two methods give the same result in the present case justifies the use of scaling for other systems.

(b) More subtle quantities, related to anomalous statistics of broad distributions, can be analysed numerically. In particular, we shall find quantities which undergo 'phase transitions' at different values of μ [9]: for instance, we shall analyse the dependence of the probability distribution of the phase φ for different frequency and μ values. A qualitative understanding of the fluctuations of the phase can be obtained (section 4): however, a quantitative treatment of this one-dimensional system (generalising existing work in localisation theory [10, 11, 14] is not yet available.

(c) From a practical point of view, the system analysed in the present paper is easy to investigate numerically: it nevertheless displays several features also encountered in more complex disordered systems. Even though one deals with very broad, 'pathological' distributions, we shall see that the admittance exponent and the phase coincide precisely with the theoretical values; the logarithmic correction term is also very clearly identified.

3. Numerical simulations

We have performed a numerical simulation in the case of the 1D chain of RC cells shown in figure 1. All capacitors are identical to a value $C = 10^{-13}$. The random resistor values $R(n)$ are chosen so that their probability distribution verified equation (1). Practically, $R(n)$ is obtained by drawing a random number $x(n)$ in the range 0 to 1 and taking $R(n) = R_0 x(n)^{-1/\mu}$ where $R_0 = 10$. The values of C and R_0 have been chosen to give a range of frequency values allowing for comparisons with analogue model systems [8].

We then compute the frequency variation for the complex admittance $A(\omega)$ between the end of the first resistor and the common ground. $A(\omega)$ is determined by a transfer matrix technique: for each cell $R(n)$, C we compute the matrix relating the inlet current and voltage $I(n)$ and $V(n)$ to the outlet values $I(n+1)$ and $V(n+1)$. These various transfer matrices are multiplied and the boundary conditions at the end point of the chain are introduced (open circuit (OC) or short circuit (CC)). Careless matrix multiplications lead quickly to numerical overflows for chain lengths as low as 50 cells: therefore the four elements of the products are multiplied by a same constant whenever needed. We keep track of these multiplicating factors which may be good indicators of the propagation of the diffusive wave into the chain. Except for $\mu=\infty$ (where R is constant), we average the values of log $|A(\omega)|$ and of the phase φ over many random choices of the set of resistors; the typical number of averages was 250 except for the critical case $\mu=1$ where 1000 realisations were performed.

3.1. Qualitative characteristics of the variations of the complex admittance

Figures 2(a) and (b) display respectively the variations of the modulus and the phase of the impedance of a chain of $N = 50\,000$ identical resistors and capacitors ($\mu=\infty$). The variations corresponding to open circuit and short circuit boundary conditions have been superimposed. At low values of the pulsation ω ($\ln\omega<0$), the lattice behaves as a single capacitor of capacitance NC (OC case) or as a single resistor of resistance NR (CC case); the corresponding limiting values of $A(\omega)$ are respectively $1/(NR)$ and $\mathrm{j}NC\omega$ with respective phases 0 and 90°. When ω increases, the penetration depth of the wave becomes of the order of the chain length and a damped pseudoresonance is observed ($1<\ln\omega<3$). At still higher ω ($3<\ln\omega<8$) the open circuit and short circuit curves become identical: $|A(\omega)|$ varies as $\sqrt{\omega}$ (slope 1/2 in the log-log plot) and the phase φ is close to 45° as expected from equation (11a). These two features are characteristic of the normal diffusion regime where the penetration depth decreases as $\omega^{-1/2}$. In the upper range of ω values ($\ln\omega>8$) the penetration depth is only one cell and $A(\omega)$ has a limit value $1/R$ with a phase $\varphi=0$. In the rest of the discussion, we shall be concerned with the diffusive region.

The overall qualitative features of the curves remain the same when μ decreases but remains higher than 1. The mean slope S of $|A(\omega)|$ in log-log coordinates in the linear part of the curve remains very close to 0.5 as can be seen in table 1. When $\mu=1$, an upward curvature of the curve is observed as expected from the prediction

$$|A(\omega)| \propto \left(\frac{\omega}{\ln \omega_0/\omega}\right)^{1/2}$$

of equation (8b) (figure 3(a)).

For $\mu<1$, one observes a clear anomalous diffusion: as in the previous case, the variation of $\log|A(\omega)|$ with ω is linear (as shown in figure 3(b) for $\mu=0.5$) but the slope is higher than 0.5.

Table 1 and figure 4(a) display the variations with μ of the slope S of numerical simulation curves such as those of figures 2(a) and 3 in the diffusion regime: we have shown for comparison the theoretical value $S_{\mathrm{th}}=1/(1+\mu)$ (for $\mu<1$). Let us point out that the two curves are slightly separated around the transition value $\mu=1$. Outside of this range, both values agree to within 1% down to $\mu=0.5$ and to 2% down to $\mu=0.25$.

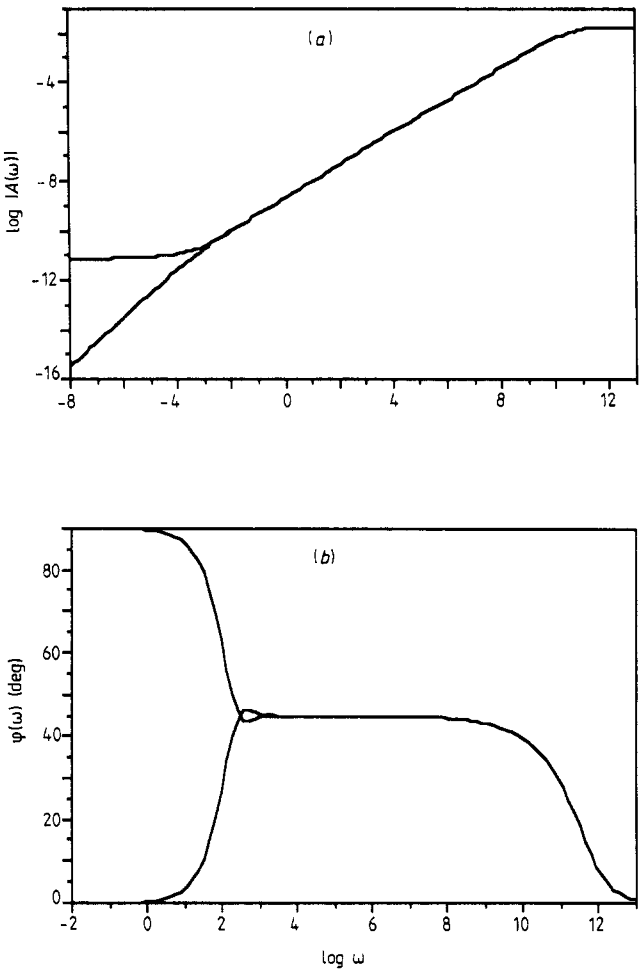

Figure 2. Frequency behaviour of the impedance in the 'pure' case ($\mu = \infty$); (a) amplitude; (b) phase.

Similar features are observed qualitatively on the variations of the phase $\overline{\varphi(\omega)}$ with frequency at different μ values (figure 5(a, b)). For all values of $\mu > 2$, the variation of $\overline{\varphi(\omega)}$ with ω is almost the same. $\overline{\varphi(\omega)}$ is close to 45° in the low frequency part of the diffusive region; it decreases at higher frequencies because of the influence of the discrete structure of the model (figure 5(a)). For $1 < \mu < 2$, there is an upward deviation (by about 1° for $\mu = 4/3$) at high frequencies from that common variation: this deviation increases as μ gets closer to 1. For $\mu < 1$, $\overline{\varphi(\omega)}$ becomes larger than 45° but the uncertainty in its value increases very fast as μ gets lower (such as for $\mu = 0.5$ in figure 5(b)).

Let us analyse now the variation with the parameter μ of the mean phase $\overline{\varphi(\omega)}$ in the diffusive regime. In order to obtain meaningful results and due to the large dispersion of the numerical values at high degrees of disorder, we averaged $\varphi(\omega)$ over 5000 realisations of the lattice; $\overline{\varphi(\omega)}$ is computed at four different frequencies in the diffusive range to estimate the dispersion of the results. Table 2 and figure 4(b) display the variations with μ of $\varphi(\omega)$ for the lowest of the four frequencies compared with

Table 1. Slope of the variation of the admittance modulus with frequency in log-log coordinates.

		Slope of $\log\|A(\omega)\|$	
μ	μ^{-1}	Numerical	Theoretical
∞	0	0.498	0.5
10	0.1	0.498	0.5
3.33	0.3	0.497	0.5
2.22	0.45	0.497	0.5
2	0.5	0.498	0.5
1.818	0.55	0.498	0.5
1.538	0.65	0.500	0.5
1.333	0.75	0.505	0.5
1.111	0.9	0.499	0.5
0.8	1.25	0.554	0.5555
0.666	1.5	0.596	0.600
0.571	1.75	0.635	0.6364
0.5	2.0	0.656	0.666
0.4	2.5	0.706	0.7142
0.333	3.0	0.743	0.750
0.286	3.5	0.769	0.7777
0.25	4.0	0.793	0.800

the theoretical value $\pi/2(1+\mu)$: this choice of frequency allows us to reduce finite size effects since the effective investigation depth is then largest. As for the slope S, the largest deviation from theory occurs near the transition value $\mu=1$; in this case, too, we think that this corresponds to a broadening of the transition due to the finite size of the lattice used. It is also around $\mu=1$ that the variations of the mean phase with frequency are highest. Far from the critical value $\mu=1$, the agreement between the theoretical and experimental values of $\varphi(\omega)$ is strikingly good, particularly at high disorders inspite of the large scatter of individual values (the error is generally less than 5%).

We have therefore shown numerically that main features such as the exponent of the variation of $|A(\omega)|$ with frequency or the mean phase value are in excellent agreement with the theoretical model. Let us now investigate more closely the critical features of the variations of the impedance near the threshold value $\mu=1$ which appeared above.

3.2. *Quantitative critical behaviour of the complex admittance near the threshold value $\mu=1$*

In order to get more precise results, we have plotted in figure 6(a) the variation of $\omega/|A(\omega)|^2$ as a function of ω in semilogarithmic coordinates for five values of $\mu=1$, 1.11, 1.205, 1.33 and 1.538. While, for $\mu=1.538$, the ratio is almost constant in the whole diffusive range, a clear linear variation is observed for $\mu=1$ with

$$\frac{\omega}{|A(\omega)|^2}=2.28\times10^{14}-1.71\times10^{13}\log_{10}\omega=1.71\times10^{13}\log_{10}\frac{2.15\times10^{13}}{\omega}. \tag{12}$$

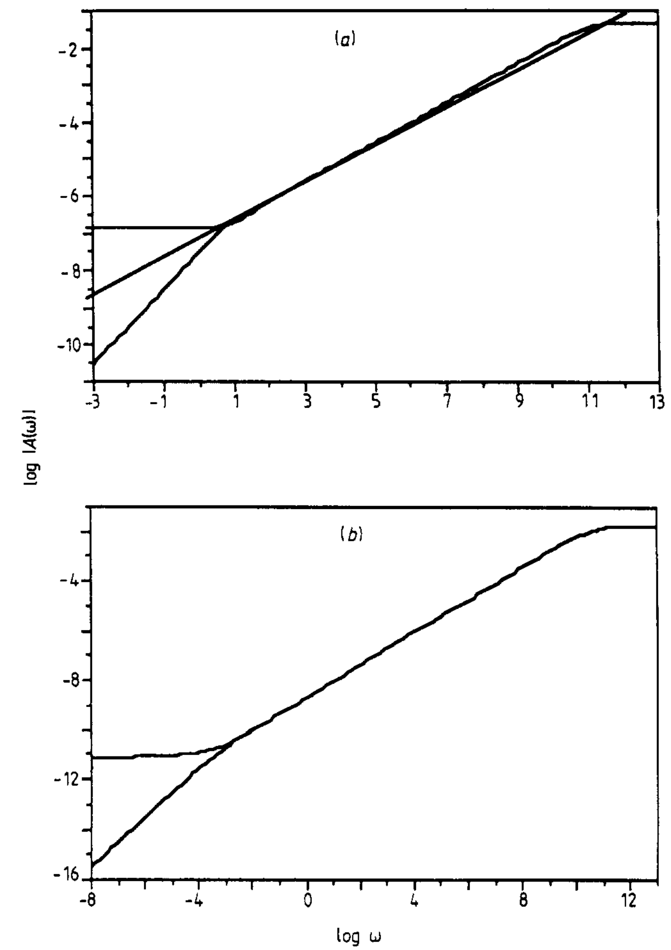

Figure 3. (*a*) Amplitude of the input impedance against frequency in a log-log plot for $\mu = 1$. Note the deviation from a straight line, indicating logarithmic corrections. (*b*) amplitude of the input impedance against frequency in a log-log plot for $\mu = 0.5$.

The parameter $\omega_0 = 2.15 \times 10^{13}$ is, as suggested above, of the order of the characteristic frequency for an individual *RC* cell. At the two intermediate values $\mu = 1.11$ and $\mu = 1.205$, $\omega/|A(\omega)|^2$ is constant at low frequencies and decreases linearly with $\log \omega$ above a threshold frequency which gets lower as μ goes towards 1. This is an indication of a broadening of the transition due to finite size effects and to the large width of the resistor distribution.

In order to make a similar analysis at $\mu < 1$, we have plotted in figure 6(*b*) the variation of $\omega/|A(\omega)|^{1+\mu}$ for $\mu = 1.0$, 0.952, 0.909, 0.854, 0.8 and 0.666; it would be a constant if $|A(\omega)|$ obeyed exactly the theoretical anomalous diffusion law. We notice that the variation of shape of the curves as μ decreases away from the transition is analogous to that observed in figure 6(*a*). For $\mu < 0.65$, the ratio $\omega/|A(\omega)|^{1+\mu}$ almost constant; for the values of μ between 0.8 and 0.95, it decreases logarithmically at high frequencies and is constant at low ones. The pretransitional effects are therefore symmetrical with respect to the transition $\mu = 1$ and are present in a limited range of μ values (typically 0.65 to 1.5).

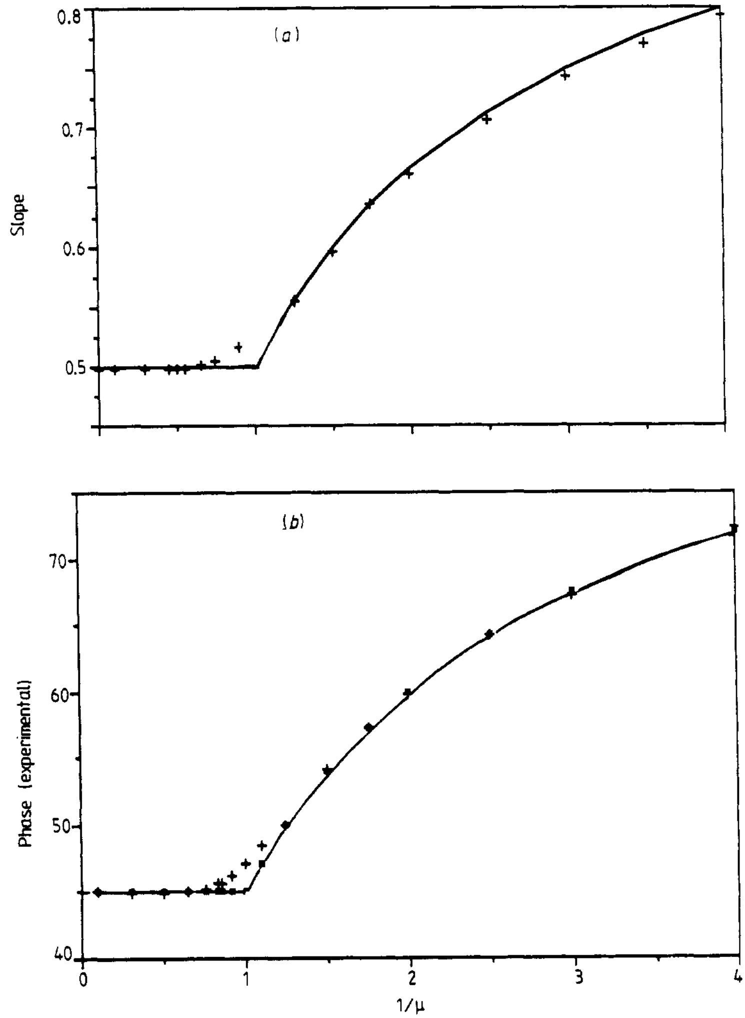

Figure 4. Numerical determination of the exponent $\partial \log A/\partial \log \omega$ and of the phase (crosses), compared with the theoretical prediction (full curves and dots). Note the finite size effects, rounding off the transition around $\mu = 1$.

4. Probability distribution of the phase of the admittance of the disordered system

4.1. Numerical results

Figures 7(a, b, c, d) shows the probability density distributions of the phase $\varphi(\omega)$ at four different values of the parameter $\mu = 2.0$, 1.0, 0.57 and 0.25. For each μ value, the histogram has been computed at four frequencies distributed over the diffusive domain.

At low degrees of disorder ($\mu > 2.0$) the probability distribution is approximately Gaussian (except at high frequencies where it becomes asymmetrical) and the width

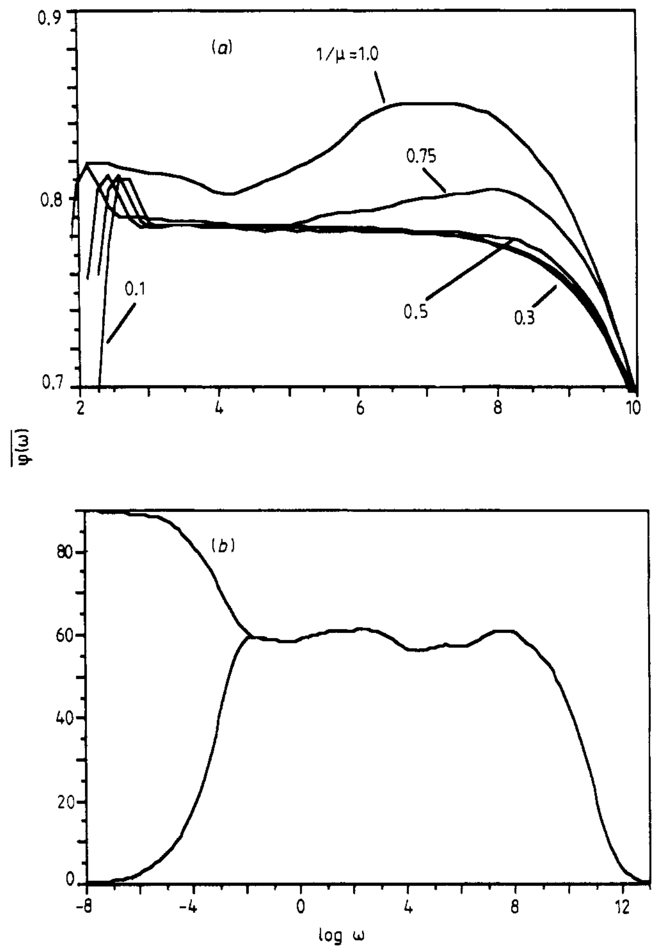

Figure 5. Variation of the average phase with frequency for several values of μ: in (a), the numbers labelling the different curves are equal to μ^{-1}, and in (b), $\mu = 0.5$.

decreases with frequency (figure 7(a)). In order to analyse this last effect, we have computed the mean square deviations $\overline{\Delta\varphi^2}$ of the phase of the admittance in our set of realisations. Figure 8(a) displays the variation of $\overline{\Delta\varphi^2}$ with frequency for different values of μ. We see that $\overline{\Delta\varphi^2}$ is proportional to $\sqrt{\omega}$ for $\mu > 2$. Between $\mu \simeq 0.65$ and $\mu \simeq 2$, $\overline{\Delta\varphi^2}$ is roughly proportional to ω^x where x gets smaller as μ decreases (however, due to the curvature of the curves, x is probably not constant). In this range the phase distribution is roughly Gaussian (figure 7(b)). At lower μ values $\leqslant 0.65$ (for instance $\mu = 0.57$ in figure 7(c)), the values of $\varphi(\omega)$ are spread over most of the total possible range (0-$\pi/2$) and the variation of $\overline{\Delta\varphi^2}$ with frequency is very slow (figure 8(c)). At very large disorders (figure 7(d)), the maximum of the distribution occurs at $\varphi = \pi/2$ with a tail at lower phase values: the tail has a smaller amplitude and decays slower when μ increases. Figure 8(b) displays the variation with $1/\mu$ of the effective exponent x obtained from a linear regression on the data of figure 8(a): x is of the order of 0.5 above $\mu = 2.0$, then it decreases steadily to zero at $\mu = 0.7$. This show that $\overline{\Delta\varphi^2}$ takes

Table 2. Variation of the first moment of the phase probability distribution with μ compared with the theoretical value.

μ	$1/\mu$	Phase (experimental)	Phase (theoretical)
10	0.1	45.000	45
3.333	0.3	44.945	45
2	0.5	44.969	45
1.538	0.65	45.070	45
1.333	0.75	45.239	45
1.204	0.83	45.635	45
1.176	0.85	45.719	45
1.086	0.92	46.297	45
1	1	47.105	45
0.909	1.1	48.432	47.142
0.8	1.25	50.016	50
0.666	1.5	54.161	54
0.571	1.75	57.320	57.272
0.5	2	59.848	60
0.4	2.5	64.343	64.285
0.333	3	67.196	67.5
0.25	4	72.272	72

an anomalous behaviour for a lower degree of disorder (corresponding to a threshold $\mu = 2.0$) than the average $\overline{\varphi(\omega)}$. Let us now theoretically investigate this problem.

4.2. *Theoretical analysis of the phase distribution*

It is a generic feature of a disordered system to exhibit different critical 'points' where different physical quantities become singular [9]. The reason for this is quite simple: if these quantities (like, e.g., the velocity and diffusion constant in a random walk problem) are the moments of a certain observable y and if this observable is broadly distributed according to $\rho(y) \simeq y^{-(1+\mu)}$, then all moments $\langle y^n \rangle$ with $n > \mu$ will be infinite, and thus lead to 'anomalous' behaviour. The analysis of the phase fluctuations will show that the simple statistical reasoning of section 2 can indeed be carried quite far. Let us recall some properties of the following sum (which have been used in section 2):

$$Y = \sum_{i=1}^{N} y_i$$

for N large and with y_i distributed according to $\rho(y)$ (and $y_i > 0$ for simplicity, see [4, 2 (appendix B)] for a more general discussion).

(a) $\mu < 1$. The quantity $Z = YN^{-1/\mu}$ has a well defined limit distribution $L_\mu(Z)$ where L_μ is a 'Levy' distribution defined by

$$L_\mu(Z) = \frac{1}{2i\pi} \int_{d-i\infty}^{d+i\infty} ds \exp[sZ - Cs^\mu].$$

L_μ itself decays asymptotically as $Z^{-(1+\mu)}$. This essentially means that Y is of order $N^{1/\mu}$ with fluctuations of the same order of magnitude.

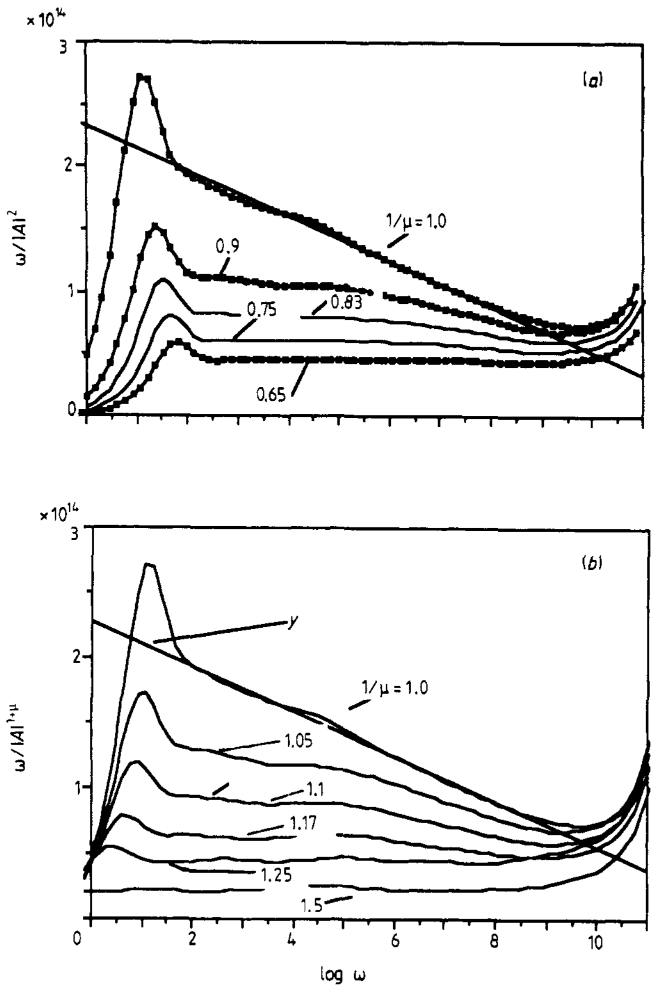

Figure 6. The logarithmic correction for $\mu = 1$ clearly evidenced by plotting ω/A^2 or $\omega/A^{1+\mu}$ against $\log \omega$ for different values of μ (the numbers given are again μ^{-1}) $y = 2.277 \times 10^{14} - 1.714 \times 10^{13} x$.

(b) $1 < \mu < 2$. The quantity which has now a well defined limit distribution is $Z = (Y - \langle y \rangle N)/N^{1/\mu}$ (this limit distribution is defined similarly to that above—see [4,2, appendix B]). Thus, now Y is of order N and its fluctuations are of order $N^{1/\mu}$.

(c) $2 < \mu$. One recovers the usual central limit theorem, for which $Z = (Y - \langle y \rangle N)/N^{1/2}$ is distributed according to a Gaussian, and hence the fluctuations are 'normal', of order $\sqrt{N}$.

For $\mu = 1$ or 2, logarithmic corrections come into play [4].

Returning to our electrical problem, this allows us to make somewhat more precise statements about the penetration depth $\lambda(\omega)$ and the admittance $A(\omega)$: since we estimate

$$\operatorname{Re} A(\omega) \approx \left[\sum^{\lambda(\omega)} R_i \right]^{-1}$$

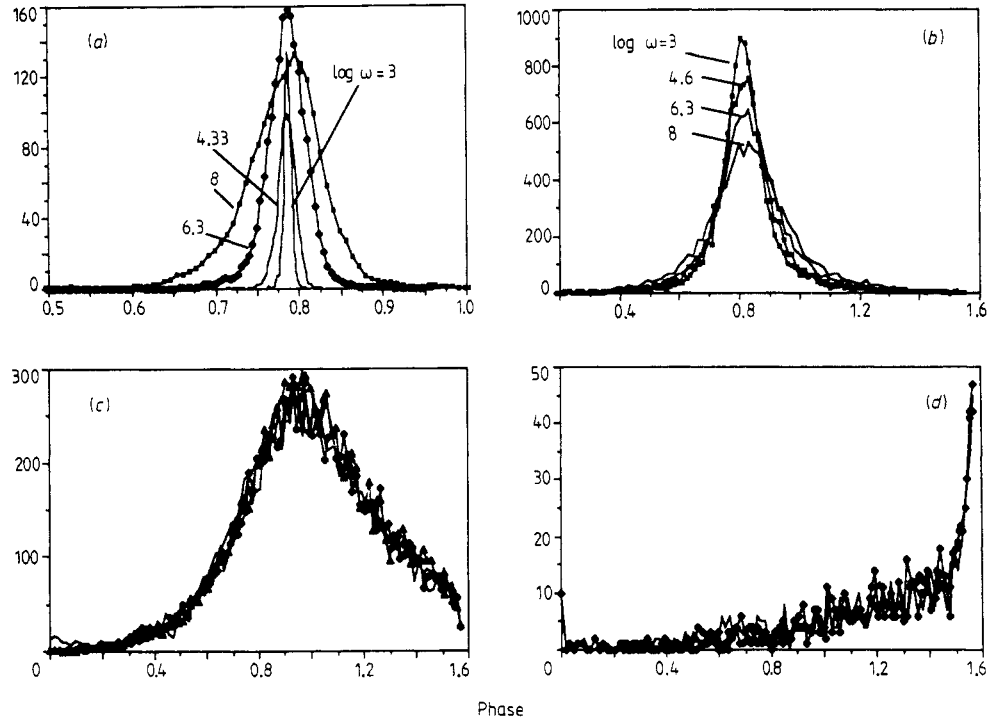

Figure 7. Phase distribution for different frequencies and $\mu =$ (*a*) 2, (*b*) 1, (*c*) 0.57, (*d*) 0.25; note that in (*a*), the vertical scale is not the same for all frequencies. The width of the distribution increases with frequency (since the penetration depth becomes smaller), as ω^x. For strong disorder, the width is of order one for any frequency ($x = 0$).

the fluctuations of the admittance come from the intrinsic fluctuation of the sum *plus* the fluctuations of its number of terms $\Delta\lambda$:

$$\Delta A \approx \begin{cases} \lambda^{1/\mu} + \Delta\lambda^{1/\mu} & \text{for } \mu < 1 \\ \lambda^{1/\mu} + \Delta\lambda & \text{for } 1 < \mu < 2 \\ \sqrt{\lambda} + \Delta\lambda & \text{for } \mu > 2. \end{cases}$$

One has

$$\frac{\Delta\lambda}{\lambda} \approx \begin{cases} 1 & \text{for } \mu < 1 \\ \omega^{(\mu-1)/2\mu} & \text{for } 1 < \mu < 2 \\ \omega^{1/4} & \text{for } \mu > 2 \end{cases}$$

which shows that (using the behaviour of $\lambda(\omega)$ of section 2) both sources of fluctuations are in fact of the same order of magnitude. Hence, finally, one has

$$\Delta\varphi = \Delta \log A = \frac{\Delta A}{A} \approx \begin{cases} 1 & \text{for } \mu < 1 \\ \omega^{(\mu-1)/2\mu} & \text{for } 1 < \mu < 2 \\ \omega^{1/4} & \text{for } \mu > 2. \end{cases}$$

This explains quantitatively the numerical results on the frequency dependence of the variance of the phase (figure 7 and figure 8 where the theoretical exponent $x = (\mu - 1)/\mu$ is compared with the numerical determination) and quantitatively the shape of the

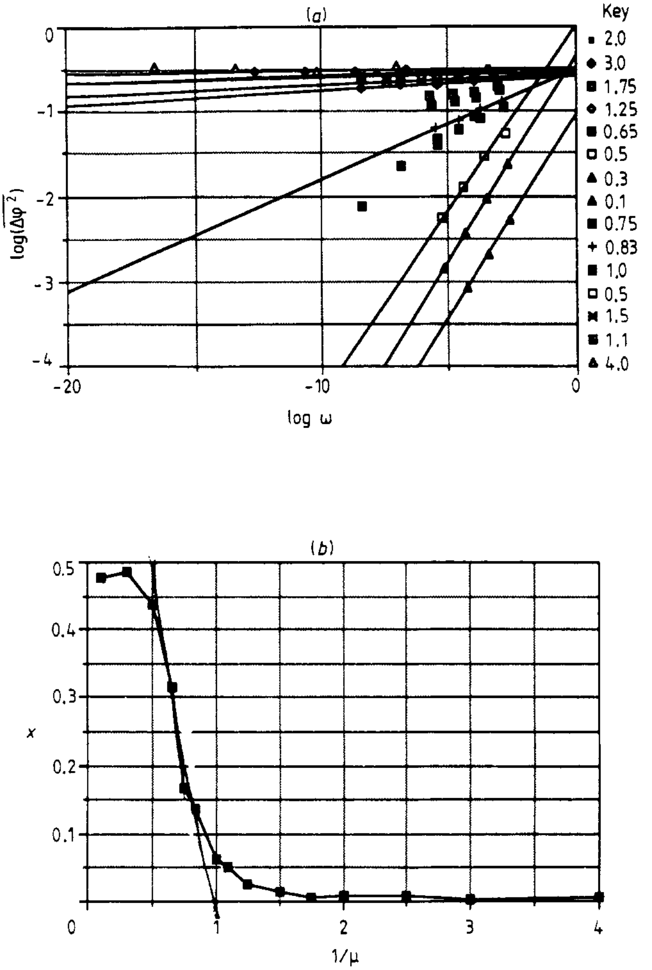

Figure 8. Exponent x against μ^{-1}: squares are numerical simulations, while the straight lines are the theoretical predictions. Agreement is quite good for this more subtle quantity. Note however again the finite size effects around the two 'transitions', $\mu = 1$ and $\mu = 2$.

whole distribution of this phase. In particular, one understands why this distribution extends over $[0, \pi]$ for $\mu < 1$ and is roughly Gaussian for $\mu > 2$. To compute precisely this distribution is far more difficult.

Our result suggests the general scaling of the phase fluctuation with frequency for, e.g., the input impedance of percolation clusters (for which broad disorder is not introduced by hand), characterised by its fractal dimension d_f and its 'spectral' dimension d_s. The mean value of the phase is known to be in that case [7, 12, 13] $\varphi = \pi d_s/4d_f$. If the electrode is a point, then

$$\Delta\varphi(\omega) \approx \omega^{d_s/4}$$

(since the number of resistors probed in a time t is $t^{d_s/2}$). If the electrode is a 'plane' of section L^{d-1}, then

$$\Delta\varphi(\omega) \approx L^{(1-d)/2}\omega^{d_s(d_f-d+1)/4d_f}.$$

5. Conclusion

We have investigated numerically the admittance of a strongly disordered chain of resistors and capacitors, and developed simple statistical arguments to understand the observed behaviour. Those arguments concern sums of broadly distributed random variables; they yield exponents which are in precise agreement with numerical data. They also justify in this case the use of a *scaling* approach. The strength of those simple arguments clearly appear when one deals with more subtle quantities such as the fluctuations of the loss angle, or logarithmic corrections to power laws, which are very satisfactorily accounted for. Two aspects should however be more precisely addressed.

As is obvious from figures 4, 7 and 8, the numerically observed exponents depart from the theoretical prediction around the 'transition points' $\mu = 1$, $\mu = 2$: the transitions are clearly rounded off by finite size effects. A detailed investigation of those has not been undertaken.

The full probability distribution of, e.g., the phase could perhaps be calculated for this one-dimensional model, as is the case for a very similar problem: the phase of the reflection coefficient for a wave arriving on a (one-dimensional) disordered medium [10, 11, 14].

Note finally that other electrical analogues of random walk problems would be worth investigating, in particular the 'random force' model which is equivalent to choosing C_n random and $R_n = (C_n C_{n+1})^{-1/2}$.

In this case $C_n = e^{U_n/kT}$ where U is the potential from which is derived the force in the random walk problem.

Acknowledgments

We wish to thank C Mitescu, E Guyon and S Roux for helpful discussions and the Schlumberger EPS-Clamart Center for letting us use their computing facilities. The work of JPH has been supported by the DRET contract 87/1406.

References

[1] Havlin S and Ben Avraham D 1987 *Adv. Phys.* **36** 695
[2] Bouchaud J P and Georges A 1990 *Phys Rep* in press
[3] Derrida B, Bouchaud J P and Georges A 1987 *Disorder and Mixing, Cargese 1987* ed E Guyon, J P Nadal and Y Pomeau (Dordrecht: Kluwer)
[4] Gnedenko B V and Kolmogorov A N 1954 *Limit distributions for sums of independent random variables* (Reading, MA: Addison-Wesley)
[5] Alexander S, Bernasconi J, Schneider W and Orbach R 1981 *Rev. Mod. Phys.* **53** 175
[6] Machta J 1985 *J. Phys. A: Math. Gen.* **18** L531
[7] Mitescu C 1988 unpublished note
[8] Rigord P and Hulin J P 1988 *Europhys. Lett.* **6** 145
[9] Derrida B 1984 *Phys. Rep.* **103** 29
[10] Sulem P L 1973 *Physica* **70** 190
[11] Bouchaud J P and Le Doussal P 1986 *J. Phys. A: Math. Gen.* **19** 797
[12] Clerc J P, Tremblay A M S, Albinet G and Mitescu C 1984 *J. Physique Lett.* **45** L913
[13] Clerc J P, Laugier J M, Girand G and Luck J M *Adv. Phys.* submitted
[14] Barnes C and Luck J M 1990 *J. Phys. A: Math. Gen.* **23** in press